Computer Networks 254 (2024) 110811

Contents lists available at ScienceDirect

Computer Networks

journal homepage: www.elsevier.com/locate/comnet

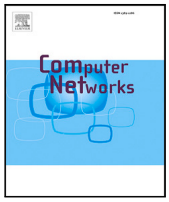

An efficient beam sweeping scheme with backup paging occasions in NR-Unlicensed Spectrum

Eshita Rastogi [a], Abhishek Roy [b], Ayush Rastogi [c], Jaehoon (Paul) Jeong [a,*], Navrati Saxena [d]

[a] Department of Computer Science and Engineering, Sungkyunkwan University, Suwon 16419, South Korea
[b] Wireless Standard Team, MediaTek USA Inc., USA
[c] System Design Lab, Networks Division, Samsung Electronics Corporation, Suwon, South Korea
[d] Department of Computer Science, San Jose State University, CA, USA

ARTICLE INFO

Keywords:
New radio
NR-Unlicensed
Full paging
Fast paging
Backup paging
Beam sweeping
Markov modeling

ABSTRACT

With the increasing demand of user applications and the shortage of cellular spectrum, New Radio (NR) access to Unlicensed Spectrum (NR-U) is getting significant attention. Listen Before Talk (LBT) procedure is used to sense unlicensed channel availability prior to transmission. The transmissions are subjected to LBT procedure failure, which brings extra delay as they are postponed to the next available transmission opportunity. This excess delay also affects time-critical procedures, such as paging. The directional communication in NR requires beamforming, which further complicates paging procedure as additional paging message transmissions are needed to cover all the beams. In this work, we propose an NR-U paging mechanism (called FF_BP) consisting of Full and Fast Paging Cycles with Backup Paging Occasions (POs). Full Paging uses a normal NR-U paging cycle and broadcasts a paging message on all the beams. On the other hand, Fast Paging, which targets delay-sensitive mobile users, uses a shorter paging cycle and broadcasts a paging message on selected beams only. The Backup POs deal with LBT procedure failure impairments while paging broadcast on selective beams reduces paging resource usage. We analyze FF_BP using a discrete-time semi-Markov chain model and validate the model by extensive simulations. The simulation results show that FF_BP outperforms several baseline mechanisms in terms of average paging delay and paging resource usage.

1. Introduction

The increasing demands of mobile applications urge the wireless vendors to explore the unlicensed spectrum to compensate for a severe shortage of the existing cellular spectrum [1,2]. To address this challenge, 3rd Generation Partnership Project (3GPP) Release 16, extended the applicability of New Radio (NR) access technology over unlicensed spectrum (NR-U) [3]. The primary objective of NR-U is to complement the existing NR to support several services in the cellular network. A critical issue is how to enable NR-U and Wi-Fi systems to reasonably coexist on a common unlicensed spectrum. To enable fair coexistence, NR-U introduces Listen Before Talk (LBT), which mandates the radio transmitter to first sense the availability of unlicensed channel before transmission [3]. Once LBT is successful, the unlicensed channel is available for a definite Maximum Channel Occupancy Time (MCOT), i.e., the maximum time the unlicensed channel can be occupied. The unavailability of unlicensed channels increases the delay in the system. The uncertainty of channel availability in the unlicensed context is likely to complicate the initial access procedures are other Medium Access Control (MAC) layer procedures in NR-U [1].

Paging is a Radio Resource Control (RRC) procedure, where the User Equipment (UE) in idle mode periodically wakes up during Paging Occasions (POs) of the Paging Frame (PF) to receive the possible paging message [4]. The use of the unlicensed spectrum complicates the paging mechanism due to necessity of LBT procedure before any Uplink (UL) and Downlink (DL) transmission. Even though a PO may be configured and the paging message is scheduled, the paging transmission by the Next Generation NodeB (gNB) is still subjected to the success of LBT procedure. Hence, depending on success or failure of the LBT procedure, the UE may or may not receive the paging from the network, respectively. When LBT procedure fails for a particular PO, the paging transmission has to be postponed, typically until the next PO. So, the UE must wait for the next scheduled PO to receive the paging message from the gNB. This degrades the system's performance by adding additional paging delay.

* Corresponding author.
E-mail addresses: eshita@skku.edu (E. Rastogi), Abhishek.Roy@mediatek.com (A. Roy), ra.ayush@samsung.com (A. Rastogi), pauljeong@skku.edu (J.(P. Jeong), navrati.saxena@sjsu.edu (N. Saxena).

https://doi.org/10.1016/j.comnet.2024.110811
Received 15 February 2024; Received in revised form 25 August 2024; Accepted 15 September 2024
Available online 19 September 2024
1389-1286/© 2024 Published by Elsevier B.V.

Additionally, in NR, the gNB is equipped with directional antennas and therefore, the paging messages are transmitted over directional links via beams. 3GPP has specified that the PO can consist of multiple time slots and paging can be transmitted by beam sweeping [4]. Thus, in order to receive the paging transmitted using beam sweeping, UE has to monitor a large number of time slots. The gNB also needs to transmit the same paging message in different directions with different beams, causing large overhead for the gNB. This exhaustive beam search also increases the delay in the system.

Considering the aforementioned scenarios, we intend to reinforce the paging mechanism for NR-U. Our proposed scheme can handle the eMBB-based applications with different delay requirements. We propose the concept of Full-Fast Paging with Backup POs (called FF_BP). In the proposed scheme, the paging message is transmitted in all directions using beam sweeping with a long DRX cycle (i.e., Full Paging) while it is transmitted only on some selected beams and directions with a short DRX cycle (i.e., Fast Paging). Fast POs are intended for delay-sensitive UEs and occur in between any two Full Paging cycles. The concept of Fast Paging helps to reduce the resource overhead for the gNB. It also reduces the beam searching time, which directly impacts the paging delay. We include additional Backup POs to cope up with the impairment caused the LBT failure. These Backup POs further reduce the average paging delay. Precisely, the major contributions of this paper are as follows:

- We propose an improvement in NR-U paging by including additional backup POs in NR-U to cope with the impairment arising from possible DL LBT failure.
- Additionally, the directional communications in NR-U also impair the performance of the paging. To deal with the overhead associated with beam sweeping and the consequent paging delay, we propose an efficient beam-sweeping Full-Fast paging with Backup POs (FF_BP). This includes the Full beam sweeping for general UEs and selected beam sweeping for the delay-sensitive UEs.
- The proposed paging mechanism is modeled using semi-Markov process. The performance of the model is evaluated in terms of paging success rate, average paging delay, and paging Resource Usage (RU), and is compared with the baseline paging mechanisms.
- Extensive simulations are carried out in MATLAB and compared with the analytical results. Performance analysis shows that the proposed mechanism outperforms the baselines in terms of average paging delay and paging RU.

The paper is organized as follows: In Section 3 we describe the proposed mechanism and discuss the system model. In Section 4, we present the modeling and analysis of the proposed paging mechanism. Section 5 describes the analytical and simulation results. Finally, Section 6 concludes our work along with the future work.

2. Related work

The regular mobility report published by Ericsson revealed that the number of mobile users are likely to surpass 5.3 billion by 2029 [5]. The escalating trend in the user demands is likely to saturate the available licensed spectrum, motivating the wireless vendors to explore unlicensed spectrum. The challenges associated with the inclusion of NR-U networks have been critically explored by the research community.

Most existing relevant studies focus on the fair coexistence of NR-U and Wi-Fi in the unlicensed spectrum. Authors in [6] propose the Markov model of NR-U and Wi-Fi coexistence system using NR-U category-4 LBT procedure and Wi-Fi Distributed Coordination Function (DCF) procedure. Authors in [7] evaluate the coexistence of NR-U and Wireless Gigabit (Wi-Gig) in mmWave by exploring different aspects such as channel access mechanism, beamforming method, numerology,

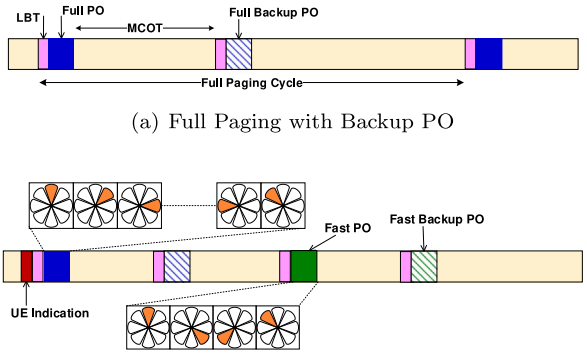

(a) Full Paging with Backup PO

(b) Full and Fast Paging with Backup PO

Fig. 1. An efficient paging mechanism with backup POs for both general UEs and delay-sensitive UEs.

etc. Similarly, authors in [8] demonstrate that the NR-U design can ensure feasible coexistence between NR-U and Wi-Gig while maintaining the Wi-Gig performance in terms of latency and throughput.

Authors in [9] leverage deep reinforcement learning to study the coexistence between the NR-U and Wi-Gig network sharing the unlicensed band to transmit data packets. However, the work does not discuss the initial access procedure needed to establish the connection between the UE and the gNB. Verboom et al. [10] introduce a stochastic model to analyze the DL performance of coexistence between Wi-Fi and NR-U in 60 GHz band. The performance is judged for severely-interfered, mildly-interfered, and not-interfered devices. With the aim to maximize the NR-U throughput, Gao et al. [11] investigate the resource allocation and interference mitigation problem between NR-U and Wi-Gig. However, the work lacks the discussion on the delay experienced by the UE in the coexistence scenario. Authors in [12–14] propose a semi-Markov based DRX model for NR-U UE to save the battery of the power-constrained mobile devices and evaluate the performance in terms of power saving and delay. But the details of initial access procedure when the UE wakes up after the sleep state are not explored.

Paging is a complicated procedure in NR-U and the directional communication further complicates and increases the resource overhead of the gNB. Therefore, resource usage becomes an important metric for discussion. Hirzallah et al. [15] provide an overview of NR-U and discuss the coexistence in 5 GHz and 6 GHz bands. They evaluate the performance in terms of throughput, latency, buffer occupancy, and channel utilization. The above mentioned research works demonstrate the co-existence of NR-U and IEEE 802.11, but none of them discuss the efficient paging scheme which can handle LBT procedure failure and reduce the delay experienced by the UE. Authors in [16] propose methods to mitigate the issues involved with peak-to-average power ratio (PAPR) to improve the QoS of the UE.

Several works investigate the directional paging operation in both LTE and NR [17,18]. However, there is limited discussion on paging in NR-U. The uncertainty of channel availability in the unlicensed band due to LBT procedure adds difficulty in sending the paging information at the pre-defined slots. The transmission of a paging message in multiple time slots is proposed in [19,20]. After the LBT procedure is successful, the gNB has multiple occasions to send paging. The user listens to all the POs, which decreases the probability of channel blocking due to channel availability but at the cost of high power consumption of the UE. Authors in [21] propose an improvement in the paging process by including additional POs, called backup POs, in the NR-U system. The backup POs are configured in such a way that it improves system performance.

We identify the following shortcomings in the current NR-U paging mechanism and observe the areas for further improvement.

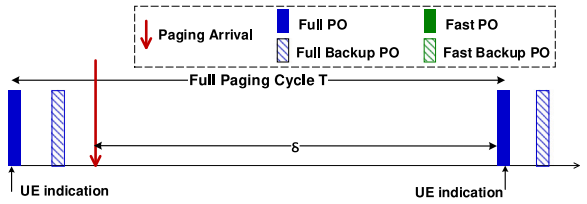

(a) $NR-U_BP$: Full Paging with Backup PO [21]

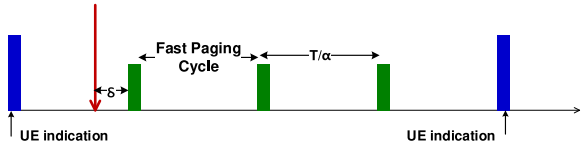

(b) FF_noBP: Full-Fast Paging without Backup PO [22]

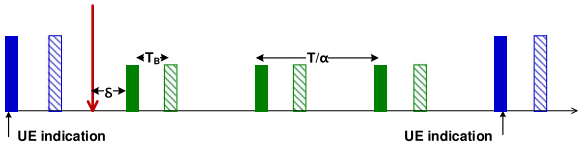

(c) FF_BP: Full-Fast Paging with Backup PO

Fig. 2. Evolution of the proposed mechanism (FF_BP).

- A substantial amount of work is done on the coexistence of NR-U with Wi-Fi and Wi-Gig, but there is limited discussion on NR-U's initial access procedure and the impact of LBT failure on it.
- Due to directional communication, the gNB has to broadcast the same paging message on all beams, which leads to the wastage of gNB's wireless resources. Since the paging messages on different beams are sent on different time-slots, it also increases the paging message transmission delay.
- The uncertainty of channel availability in the unlicensed spectrum due to LBT procedure complicates the paging procedure by making the paging information difficult to send at pre-defined time slots.
- Since both the DL and UL transmissions in NR-U are subjected to LBT failure, this adds extra delay to the system, making the paging framework inefficient.

In this work, we attempt to investigate the aforementioned concerns and redesign the paging framework for NR-U. Overall, our proposed scheme, FF_BP, intend to decrease the radio resource overhead for the gNB and the average paging delay. To the best of our knowledge, the paging framework for NR-U to cope with the LBT procedure failure is yet to be explored.

3. Proposed paging mechanism and system model

In this section, we discuss our proposed paging mechanism, followed by the system model used to model and analyze this proposed mechanism.

3.1. Proposed paging mechanism

Paging is a Radio Resource Control (RRC) procedure, where the UE in idle mode periodically wakes up during POs of the PF to receive paging. The use of unlicensed spectrum complicates the paging mechanism. In NR-U, for any UL or DL transmission, the LBT procedure is performed to know the availability of unlicensed channel. These transmissions are occasionally subjected to LBT failure and the UE may or may not receive paging from the network. So, the UE must wait for the next scheduled PO to receive the paging message from the gNB. This degrades the system's performance by adding paging delay. Fig. 1 explains an efficient paging mechanism (FF_BP) proposed in this paper.

To deal with the impairment caused by the LBT failure, we enhance the legacy NR-U paging mechanism into an efficient NR-U paging mechanism by providing a backup PO soon after the regular NR-U PO, as shown in Fig. 1(a) [21]. After the regular NR-U PO, the gNB should wait for at least MCOT to schedule the backup PO. This is essential to maintain a fair coexistence between the cellular UEs using the unlicensed spectrum and the Wi-Fi UEs. To avoid continuous listening to backup POs, a UE does not need to monitor a backup PO if it receives a paging message in the associated regular NR-U PO.

Additionally, the cellular network comprises of multiple types of UEs with different delay requirements. In this work, we primarily consider two types of UEs: (i) general UEs, which do not have stringent delay requirements, and (ii) delay-sensitive UEs, which have stricter delay requirements than general UEs. Both these UE types generally fall into the category of enhanced Mobile Broadband (eMBB) services. The paging to general UEs is sent on POs defined in the current 3GPP NR-U paging mechanism and is broadcasted on all the beams using beam sweeping, as shown in Fig. 1(b). Therefore, we term this paging as Full Paging.

Considering the effect of directional communication, the gNB has to broadcast the paging messages on all the beams. It is inefficient to spend additional resources on exhaustive beam sweeping because it increases the resource overhead for the gNB, besides adding extra delay in overall paging process, which is not desirable of the delay-sensitive UEs. Therefore, we consider a Fast Paging mechanism in which the paging is sent using a shorter paging cycle to delay-sensitive UEs over some selected beams, as shown in Fig. 1(b). We note that the paging is sent to a delay-sensitive UE on a Full PO also, if the Full PO occurs soon after a paging request for this UE has been received. To facilitate the gNB in sending Fast Paging over selected beams, the delay-sensitive UEs send an indication of their best beam just before every Full PO. Then, until the next Full PO, the gNB sends Fast Paging on only the selected beams. Further, since Fast Paging may also suffer from LBT failures, each Fast PO is also associated with a backup PO.

Overall, we believe that the introduction of backup PO for both Full and Fast Paging, as shown in Fig. 1(b), will help to overcome the impairment caused by LBT failure by reducing the paging delay for the UEs and improving the paging RU of the gNB. Note that Fig. 2 illustrates the evolution of the proposed paging mechanism (FF_BP) through two baseline paging mechanisms.

3.2. System model and problem formulation

We consider a coexistence scenario consisting of n_w Wi-Fi Access Points (APs) and n_l NR-U gNBs sharing the unlicensed spectrum for DL data transmission. The system model consists of N UEs uniformly distributed within the cell. All the Wi-Fi and cellular nodes are assumed to co-exist in the same frequency band. We consider standalone deployment mode for NR-U, where the unlicensed band is used for both control signal and data transmission. The gNB uses the category-4 LBT procedure before DL transmission to initiate a Channel Occupancy Time (COT) [22] while the APs use the Wi-Fi DCF mechanism. The UE is always mandated to perform category-2 or category-1 LBT procedure prior to any UL transmission, such as feedback signals.

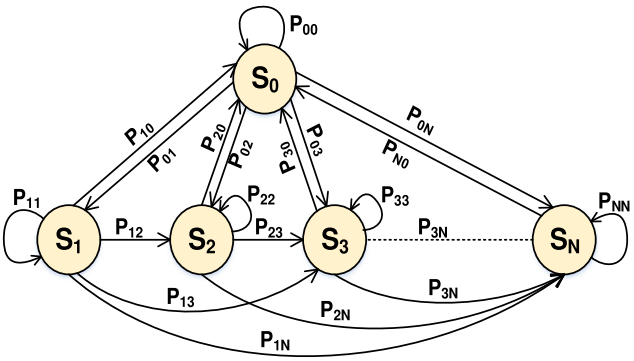

Fig. 3. Semi-Markov modeling of full paging without backup PO.

3.2.1. Modeling of LBT procedure

The channel access mechanism adopted by 3GPP is based on a Clear Channel Assessment (CCA) procedure that uses LBT procedure in compliance with the European Telecommunications Standards Institute (ETSI) regulations. We use an LBT-category 4 procedure with the random backoff [23]. A gNB adopts a random backoff mechanism and uses a backoff counter to avoid a collision that is caused by two or more nodes transmitting simultaneously. Once the channel is available, the transmitter can use the channel for a maximum time referred to as MCOT. The LBT procedure in our work is modeled as described in [23].

3.2.2. Modeling of Wi-Fi DCF procedure

The Wi-Fi DCF procedure is described using the classical 2-dimensional Markov model [24]. According to [24], the probability that a Wi-Fi AP transmits a data packet is calculated as:

$$\tau_w = \frac{2(1-2p_{w,c})}{(1-2p_{w,c})(W_{w,0}+1)+p_{w,c}W_{w,0}[1-(2p_{w,c})^{m_w}]}, \tag{1}$$

where $p_{w,c}$ is the probability that a collision occurs when Wi-Fi AP transmits a data packet in a slot, $W_{w,0}$ is the minimum contention window in Wi-Fi DCF, and m_w is the maximum backoff stage in Wi-Fi DCF.

4. Modeling and analysis of paging in NR-U

In this section, we present the modeling of our proposed paging framework. In the following subsections, we first model the paging mechanism without backup paging, followed by the paging mechanism with backup paging. Finally, we derive the overall analytical formulation for the system model.

4.1. Paging mechanism without backup paging

We model the paging mechanism using a discrete-time semi-Markov chain, where the current state is used to predict the future state and the states are updated the end of each PO. The semi-Markov process is used to define transition probability from one state to another [25,26]. This model is used because the decision for the number of UEs for which paging is required in a PO depends only on the previous PO and not on the POs before that. Also, the transition time from one state to the next is fixed by the paging cycle of the UEs. This is in contrast to a Markov process, where transition times are exponentially-distributed.

Fig. 3 illustrates the model of the paging mechanism without backup paging. We note that the following analysis applies to both Full Paging as well as Fast Paging. The only difference for Fast Paging is that the paging cycle changes from T to T/α, where α is the Fast Paging Cycle Factor (FPCF), and the number of UEs changes from N to $N' = \sigma N$, where $0 < \sigma < 1$. We consider that paging requests per UE are generated according to a Poisson process with arrival rate (λ). We denote the DL LBT success probability by ρ. DL transmission is only possible when the LBT performed by the gNB is successful; otherwise, the UE has to wait until the gNB's LBT is successful.

In the state diagram shown in Fig. 3, state S_M $(0 \le M \le N)$ means that the gNB needs to send paging to M UEs in the next PO. The gNB state is updated at the end of each PO. Due to Poisson arrivals, the probability of no paging arrival for a UE during a paging cycle is given by $e^{-\lambda T}$ and the probability of at least 1 paging arrival for a UE during a paging cycle is given by $\left(1-e^{-\lambda T}\right)$. Let P_{ij} be the transition probability from state S_i to state S_j. The transition $S_0 \longrightarrow S_0$ occurs when either there is no paging arrival in a time period T or there is paging arrival for at least 1 UE in a time period T, followed by DL LBT success at the next PO. So, the transition probability P_{00} is given by

$$P_{00} = e^{-\lambda NT} + \left(1-e^{-\lambda NT}\right)\rho. \tag{2}$$

The transition $S_0 \longrightarrow S_M, 0 < M \le N$, occurs when there is paging arrival for M UEs in a time period T, followed by DL LBT failure at the next PO. The probability of paging arrival for M UEs in a time period T is ${}^{N}\mathrm{C}_{\mathrm{M}}\left(1-\mathrm{e}^{-\lambda \mathrm{T}}\right)^{\mathrm{M}}\left(\mathrm{e}^{-\lambda \mathrm{T}}\right)^{\mathrm{N-M}}$, where ${}^{N}\mathrm{C}_{\mathrm{M}}$ denotes the number of possible ways of selecting M UEs out of N UEs. Since the DL LBT failure probability is $(1-\rho)$, the transition probability P_{0M} is given by

$$P_{0M} = {}^{N}\mathrm{C}_{\mathrm{M}}\left(1-\mathrm{e}^{-\lambda \mathrm{T}}\right)^{\mathrm{M}}\left(\mathrm{e}^{-\lambda \mathrm{T}}\right)^{\mathrm{N-M}}(1-\rho), \tag{3}$$

where $0 < M \le N$. The transition $S_M \longrightarrow S_0, 0 < M \le N$, occurs when there is DL LBT success at the next PO. So, the transition probability P_{M0} is given by ρ. The transition $S_M \longrightarrow S_{M'}, 0 < M \le N, M \le M' \le N$, occurs when there is paging arrival for at least 1 UE in a time period T, followed by DL LBT failure at the next PO. So, the transition probability $P_{MM'}$ is given by

$$P_{MM'} = (1-\rho)\,{}^{N-M}\mathrm{C}_{\mathrm{M'-M}}\left(1-\mathrm{e}^{-\lambda \mathrm{T}}\right)^{\mathrm{M'-M}}\left(\mathrm{e}^{-\lambda \mathrm{T}}\right)^{\mathrm{N-M'}}. \tag{4}$$

Let π_{Fu_M} denote the steady state probability of the state S_M, $0 \le M \le N$, of the semi-Markov chain. First, using balance equations, we calculate π_{Fu_0} as

$$\begin{aligned}\pi_{Fu_0} &= \pi_{Fu_0}P_{00} + \pi_1 P_{10} + \pi_2 P_{20} + \cdots + \pi_N P_{N0} \\ &= \pi_{Fu_0}P_{00} + \rho\sum_{n=1}^{N}\pi_n.\end{aligned} \tag{5}$$

Substituting the value of P_{00} from (2) and using $\sum_{n=0}^{N}\pi_n = 1$, we calculate π_{Fu_0} as

$$\pi_{Fu_0} = \frac{\rho}{1-(1-\rho)e^{-\lambda NT}}. \tag{6}$$

Next, using balance equations, we calculate $\pi_{Fu_M}, 0 < M \le N$ as

$$\begin{aligned}\pi_{Fu_1} &= \pi_{Fu_0}P_{01} + \pi_{Fu_1}P_{11} \\ \pi_{Fu_2} &= \pi_{Fu_0}P_{02} + \pi_{Fu_1}P_{12} + \pi_{Fu_2}P_{22} \\ \pi_{Fu_3} &= \pi_{Fu_0}P_{02} + \pi_{Fu_1}P_{12} + \pi_{Fu_2}P_{22} + \pi_{Fu_3}P_{33} \\ &\vdots\end{aligned} \tag{7}$$

So, in general, we can write π_{Fu_M} as

$$\begin{aligned}\pi_{Fu_M} &= \sum_{n=0}^{M-1}\pi_{Fu_n}P_{nM} + \pi_{Fu_M}P_{MM} \\ &= \frac{\sum_{n=0}^{M-1}\pi_{Fu_n}P_{nM}}{1-P_{MM}}\end{aligned} \tag{8}$$

Similarly, for Fast Paging,

$$\pi_{Fa_0} = \frac{\rho}{1-(1-\rho)e^{-\lambda N'(T/\alpha)}} \tag{9}$$

and

$$\pi_{Fa_M} = \frac{\sum_{n=0}^{M-1}\pi_{Fa_n}P_{nM}}{1-P_{MM}}; 0 < M \le N'. \tag{10}$$

4.1.1. Paging success rate

We define the paging success rate as the ratio of the number of successful paging transmissions (i.e., DL LBT was successful) to the number of attempted paging transmissions. Suppose, at the end of current PO, the gNB is in state S_M with probability π_{Fu_M}, which means that the gNB has to send paging to M UEs in the next PO. However, there can be additional paging arrivals for the remaining $(N-M)$ UEs in the paging cycle of duration T between the current and the next PO. Out of the remaining $(N-M)$ UEs, the probability of paging arrivals for M' UEs, $0 \le M' \le (N-M)$, is given by ${}^{N-M}\mathrm{C}_{\mathrm{M}'}\left(1-\mathrm{e}^{-\lambda \mathrm{T}}\right)^{\mathrm{M}'}\left(\mathrm{e}^{-\lambda \mathrm{T}}\right)^{\mathrm{N-M-M}'}$. So, in the next PO, the gNB needs to send paging to $(M+M')$ UEs, where $M \le (M+M') \le N$. Since the DL LBT success probability is ρ, the paging success rate by summing over all possible gNB states is given by

$$\begin{aligned}\Gamma_{Fu} &= \sum_{M=0}^{N} \rho \pi_{Fu_M} \sum_{M'=0}^{N-M} {}^{N-M}\mathrm{C}_{\mathrm{M}'}\left(1-\mathrm{e}^{-\lambda \mathrm{T}}\right)^{\mathrm{M}'} \left(e^{-\lambda T}\right)^{N-M-M'} \\ &= \rho \sum_{M=0}^{N} \pi_{Fu_M} \left(1-e^{-\lambda T}+e^{-\lambda T}\right)^{N-M} \\ &= \rho \sum_{M=0}^{N} \pi_{Fu_M} \\ &= \rho. \end{aligned} \tag{11}$$

From the above equation, we see that the paging success rate is equal to the DL LBT success probability. This means the paging success rate cannot be more than the DL LBT success probability because the channel can only be occupied when the DL LBT is successful. Following a similar analysis, we can show that paging success rate for Fast Paging is also ρ.

4.1.2. Paging resource usage (RU)

Let us assume that a single resource unit is used to send paging to one UE in one beam. If the gNB has B beams, MB resources units are used to send Full Paging to M UEs on B beams. So, the average resource units used to send Full Paging in one PO are

$$\Omega_{Fu} = B \sum_{M=0}^{N} M \ \pi_{Fu_M}. \tag{12}$$

The gNB sends Fast Paging only on the preferred beams indicated by delay-sensitive UEs before each Full PO. If the number of delay-sensitive UEs is less than the number of beams (i.e., $N' < B$), then the gNB can receive an indication on maximum N' beams because each UE indicates only 1 beam as its best beam. However, if $N' \ge B$, then the gNB may receive an indication for all the beams in the system and hence, Fast Paging may be required on maximum B beams. So, the maximum number of beams used for Fast Paging transmission is given by $min(B, N')$. Thus, the maximum resource units used to send Fast Paging in one PO are

$$\Omega_{Fa} = min(B, N') \sum_{M=0}^{N'} M \ \pi_{Fa_M}. \tag{13}$$

4.1.3. Average paging delay

The paging delay experienced by a UE is the time-difference from the time the gNB receives a paging request for the UE from the core network to the time the gNB successfully transmits a paging request to the UE. Fig. 4(a) illustrates the paging delay experienced by a UE in Full Paging without Backup POs. For Full Paging, if the paging is successful at the first, the second, or the third transmission attempt, the paging delay is $\delta\ \rho$, $(\delta+T)\ (1-\rho)\rho$, or $(\delta+2T)\ (1-\rho)^2\rho$, respectively.

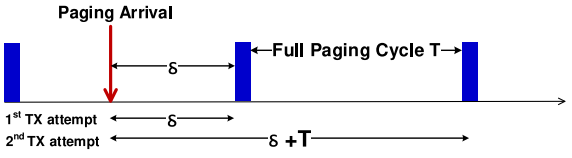

(a) Full Paging with no Backup PO

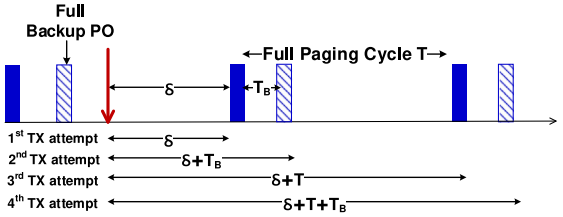

(b) Full Paging with Backup PO

Fig. 4. Illustration of delay calculation for NR-U paging.

Since the gNB attempts to page the UE until the paging request is sent successfully, the average paging delay is expressed as

$$\begin{aligned}\Delta_{Fu} &= \sum_{k=0}^{\infty} (\delta + kT)\ (1-\rho)^k\ \rho \\ &= \delta\ \rho \sum_{k=0}^{\infty} (1-\rho)^k + T\ \rho \sum_{k=0}^{\infty} k\ (1-\rho)^k \\ &= \frac{\delta\rho}{\rho} + \frac{T\ \rho\ (1-\rho)}{\rho^2} \\ &= \delta + T\ \left(\frac{1}{\rho} - 1\right). \end{aligned} \tag{14}$$

Assuming that δ is uniformly distributed in $[0, T]$ and substituting δ with its average value of $T/2$, the expression for Δ_{Fu} is simplified as

$$\Delta_{Fu} = \frac{T}{\rho} - \frac{T}{2}. \tag{15}$$

From the above equation, it is seen that the average paging delay depends on the Full Paging cycle and the DL LBT success probability. The average paging delay for Fast Paging without Backup Paging is similarly expressed as

$$\Delta_{Fa} = \frac{T}{\alpha\rho} - \frac{T}{2\alpha}. \tag{16}$$

4.2. Paging mechanism with backup paging

In this model, a state $S_{Fu_M, FuB_{M'}, next\ PO\ type}$ is defined as the state in which Full Paging is required for M UEs $(0 \le M \le N)$, Backup Paging is required for M' UEs $(0 \le M' \le N)$, and the next PO type is either a Full PO or a Backup PO. Since state transitions depend only on the previous state and the transition time from one state to the next is fixed by the paging cycle of the UEs, we model it by a discrete-time semi-Markov chain. Table 1 shows the possible state transitions, and the corresponding transition events and transition probabilities. Fig. 5 illustrates the model of the paging mechanism with backup paging. As shown in Table 1, the possible states are

- $S_{Fu_M, FuB_0, Full\ PO}, 0 \le M \le N$ and
- $S_{Fu_M, FuB_{M'}, Backup\ PO}, 0 \le M' \le N-M, 0 \le M \le N$.

The stationary distribution of the semi-Markov Chain is given by Eqs. (17)–(22) given in Box I.

Using the transition probabilities shown in Table 1, the balance equations for the steady-state probabilities are given by Eqs. (18)

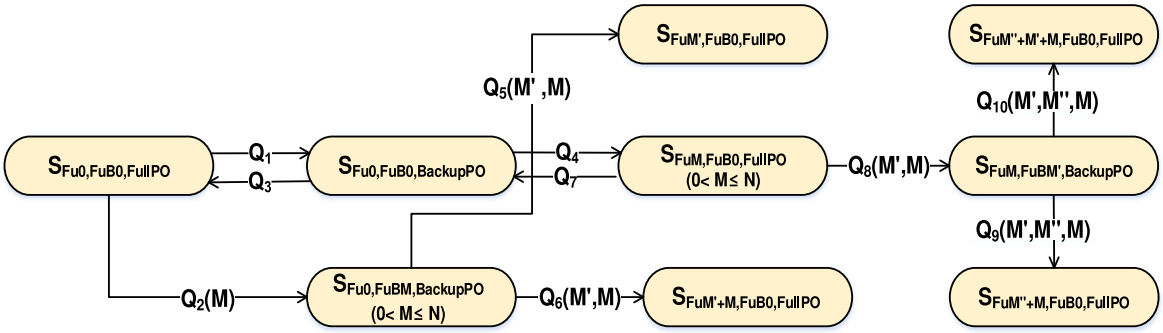

Fig. 5. Semi-Markov modeling of full paging with backup PO.

Table 1
Transition probabilities in full paging with backup PO.

State transitions	Transition events	Transitions probabilities
$\{S_{Fu_0,FuB_0,FullPO}\} \longrightarrow \{S_{Fu_0,FuB_0,BackupPO}\}$	No paging arrivals in time-period $(T-T_B)$ or paging arrival for at least 1 UE in time-period $(T-T_B)$, followed by DL LBT success at next PO	$Q_1 = e^{-\lambda N(T-T_B)} + \left(1-e^{-\lambda N(T-T_B)}\right)\rho$
$\{S_{Fu_0,FuB_0,FullPO}\} \longrightarrow \{S_{Fu_0,FuB_M,BackupPO}\}$	Paging arrival for M UEs in time-period $(T-T_B)$, followed by DL LBT failure at next PO	$Q_2(M) = {}^{N}\mathrm{C}_{\mathrm{M}}\left(1-\mathrm{e}^{-\lambda(\mathrm{T}-\mathrm{T_B})}\right)^{M}\left(\mathrm{e}^{-\lambda(\mathrm{T}-\mathrm{T_B})}\right)^{\mathrm{N}-\mathrm{M}}(1-\rho);$ $0 < M \le N$
$\{S_{Fu_0,FuB_0,BackupPO}\} \longrightarrow \{S_{Fu_0,FuB_0,FullPO}\}$	No paging arrivals in time-period T_B	$Q_3 = e^{-\lambda N T_B}$
$\{S_{Fu_0,FuB_0,BackupPO}\} \longrightarrow \{S_{Fu_M,FuB_0,FullPO}\}$	Paging arrival for M UEs in time-period T_B	$Q_4(M) = {}^{N}\mathrm{C}_{\mathrm{M}}\left(1-\mathrm{e}^{-\lambda \mathrm{T_B}}\right)^{\mathrm{M}}\left(\mathrm{e}^{-\lambda \mathrm{T_B}}\right)^{\mathrm{N}-\mathrm{M}};$ $0 < M \le N$
$\{S_{Fu_0,FuB_M,BackupPO}\} \longrightarrow \{S_{Fu_{M'},FuB_0,FullPO}\}$	Paging arrival for M UEs in time-period T_B, followed by DL LBT success at the next PO	$Q_5(M',M) = {}^{N-M}\mathrm{C}_{\mathrm{M}'}\left(1-\mathrm{e}^{-\lambda \mathrm{T_B}}\right)^{\mathrm{M}'}\left(\mathrm{e}^{-\lambda \mathrm{T_B}}\right)^{\mathrm{N}-\mathrm{M}-\mathrm{M}'}\rho;$ $0 \le M' \le N-M, 0 < M \le N$
$\{S_{Fu_0,FuB_M,BackupPO}\} \longrightarrow \{S_{Fu_{M'+M},FuB_0,FullPO}\}$	Paging arrival for M' in time-period T_B UEs, followed by DL LBT failure at next PO	$Q_6(M',M) = {}^{N-M}\mathrm{C}_{\mathrm{M}'}\left(1-\mathrm{e}^{-\lambda \mathrm{T_B}}\right)^{\mathrm{M}'}\left(\mathrm{e}^{-\lambda \mathrm{T_B}}\right)^{\mathrm{N}-\mathrm{M}-\mathrm{M}'}(1-\rho);$ $0 \le M' \le N-M, 0 < M \le N$
$\{S_{Fu_M,FuB_0,FullPO}\} \longrightarrow \{S_{Fu_0,FuB_0,BackupPO}\}$	No paging arrivals or paging arrival for at least 1 UE in time-period $(T-T_B)$, followed by DL LBT success at the next PO	$Q_7 = \rho$
$\{S_{Fu_M,FuB_0,FullPO}\} \longrightarrow \{S_{Fu_M,FuB_{M'},BackupPO}\}$	Paging arrival for M' UEs in time-period $(T-T_B)$, followed by DL LBT failure at next PO	$Q_8(M',M) = {}^{N-M}\mathrm{C}_{\mathrm{M}'}\left(1-\mathrm{e}^{-\lambda(\mathrm{T}-\mathrm{T_B})}\right)^{\mathrm{M}'}\left(\mathrm{e}^{-\lambda(\mathrm{T}-\mathrm{T_B})}\right)^{\mathrm{N}-\mathrm{M}-\mathrm{M}'}(1-\rho);$ $0 \le M' \le N-M, 0 < M \le N$
$\{S_{Fu_M,FuB_{M'},BackupPO}\} \longrightarrow \{S_{Fu_{M''+M},FuB_0,FullPO}\}$	Paging arrival for M'' UEs in time-period T_B, followed by DL LBT success at the next PO	$Q_9(M'',M',M) = {}^{N-M-M'}\mathrm{C}_{\mathrm{M}''}\left(1-\mathrm{e}^{-\lambda \mathrm{T_B}}\right)^{\mathrm{M}''}\left(\mathrm{e}^{-\lambda \mathrm{T_B}}\right)^{\mathrm{N}-\mathrm{M}-\mathrm{M}'-\mathrm{M}\varepsilon}\rho;$ $0 \le M'' \le N-M-M', 0 \le M' \le N-M, 0 < M \le N$
$\{S_{Fu_M,FuB_{M'},BackupPO}\} \longrightarrow \{S_{Fu_{M''+M'+M},FuB_0,FullPO}\}$	Paging arrival for M'' UEs in time-period T_B, followed by DL LBT failure at next PO	$Q_{10}(M'',M',M) = {}^{N-M-M'}\mathrm{C}_{\mathrm{M}''}\left(1-\mathrm{e}^{-\lambda \mathrm{T_B}}\right)^{\mathrm{M}''}\left(\mathrm{e}^{-\lambda \mathrm{T_B}}\right)^{\mathrm{N}-\mathrm{M}-\mathrm{M}'-\mathrm{M}\varepsilon}(1-\rho);$ $0 \le M'' \le N-M-M', 0 \le M' \le N-M, 0 < M \le N$

through (22). The transition probability matrix of the semi-Markov Chain, Q, is derived from these balance equations. Further, from the definition of the stationary distribution of a semi-Markov Chain, $\Pi_{Fu}Q = \Pi_{Fu}$, and Π_{Fu} is derived by solving this equation numerically. We note that the above analysis applies to both Full Paging as well as Fast Paging. The only difference for Fast Paging is that the paging cycle changes from T to T/α, where α is the FPCF, and the number of UEs changes from N to N'. The possible states for the semi-Markov Chain for Fast Paging are

- $S_{Fa_M,FaB_0,Full\ PO}, 0 \le M \le N'$ and
- $S_{Fa_M,FaB_{M'},Backup\ PO}, 0 \le M' \le N'-M, 0 \le M \le N'$.

The stationary distribution of the semi-Markov Chain for Fast Paging is given by

$$\begin{aligned}\Pi_{Fa} = [&\pi_{Fa_0,FaB_0,Full\ PO}\\ &\vdots\\ &\pi_{Fa_N,FaB_0,Full\ PO}\\ &\pi_{Fa_0,FaB_0,Backup\ PO}\\ &\vdots\\ &\pi_{Fa_0,FaB_N,Backup\ PO}\\ &\pi_{Fa_1,FaB_0,Backup\ PO}\\ &\vdots\\ &\pi_{Fa_1,FaB_{N-1},Backup\ PO}\\ &\vdots\\ &\pi_{Fa_N,FaB_0,Backup\ PO}]\end{aligned} \tag{23}$$

As explained above, the balance equations for Fast Paging are obtained by replacing T with T/α and N with N' in Eqs. (18) through (22). After that, the transition probability matrix and Π_{Fa} are also obtained in the same way as for Full Paging.

4.2.1. Paging success rate

We define the paging success rate as the ratio of the number of successful paging transmissions (i.e., DL LBT was successful) to the

$$\Pi_{Fu} = [\pi_{Fu_0,FuB_0,Full\ PO} \vdots \pi_{Fu_N,FuB_0,Full\ PO} \pi_{Fu_0,FuB_0,Backup\ PO} \vdots \pi_{Fu_0,FuB_N,Backup\ PO} \pi_{Fu_1,FuB_0,Backup\ PO} \vdots \pi_{Fu_1,FuB_{N-1},Backup\ PO} \vdots \pi_{Fu_N,FuB_0,Backup\ PO}] \tag{17}$$

$$\pi_{Fu_0,FuB_0,Backup\ PO} = Q_1\pi_{Fu_0,FuB_0,Full\ PO} + Q_7\sum_{M=1}^{N}\pi_{Fu_M,FuB_0,Full\ PO}. \tag{18}$$

$$\pi_{Fu_0,FuB_M,Backup\ PO} = Q_2(M)\pi_{Fu_0,FuB_0,Full\ PO}, 1 \le M \le N. \tag{19}$$

$$\pi_{Fu_M,FuB_{M'},Backup\ PO} = Q_8(M',M)\pi_{Fu_M,FuB_0,Full\ PO}, 0 \le M' \le N-M \text{ and } 1 \le M \le N. \tag{20}$$

$$\pi_{Fu_0,FuB_0,Full\ PO} = Q_3\pi_{Fu_0,FuB_0,Backup\ PO} + \sum_{M=1}^{N} Q_5(0,M)\pi_{Fu_0,FuB_M,Backup\ PO}. \tag{21}$$

$$\pi_{Fu_J,FuB_0,Full\ PO} = Q_4(J)\pi_{Fu_0,FuB_0,Backup\ PO} + \sum_{M=1}^{N-J} Q_5(J,M)\pi_{Fu_0,FuB_M,Backup\ PO} + \sum_{M=1}^{J} Q_6(J-M,M)\pi_{Fu_0,FuB_M,Backup\ PO} + \sum_{M=1}^{J}\sum_{M'=0}^{N-M} Q_9(J-M,M',M)\pi_{Fu_M,FuB_{M'},Backup\ PO} + \sum_{M=1}^{J}\sum_{M'=0}^{J-M} Q_{10}(J-M'-M,M',M)\pi_{Fu_M,FuB_{M'},Backup\ PO}, 1 \le J \le N. \tag{22}$$

Box I.

number of attempted paging transmissions. Suppose, at the end of current Full PO, the gNB is currently in state $S_{Fu_M,FuB_{M'},BackupPO}$ with probability $\pi_{Fu_M,FuB_{M'},Backup\ PO}$, which means that the gNB has to send paging to $(M+M')$ UEs in the next Backup PO. However, there can be additional paging arrivals for the remaining $(N-M-M')$ UEs in the paging cycle of duration T_B between the current Full PO and the next Backup PO. Out of the remaining $(N-M-M')$ UEs, the probability of paging arrivals for M'' UEs, $0 \le M'' \le (N-M-M')$, is given by $\pi_{Fu_M,FuB_{M'},Backup\ PO}\ {}^{N-M-M'}\mathrm{C}_{M''}\left(1-\mathrm{e}^{-\lambda T_B}\right)^{M''}\left(\mathrm{e}^{-\lambda T_B}\right)^{N-M-M'-M''}$. So, in the next PO, the gNB needs to send paging to $(M+M'+M'')$ UEs, where $M+M' \le (M+M'+M'') \le N$. Following a similar reasoning for all possible states, the paging success rate by summing over all the possible gNB states, Γ_{Fu}^{BP}, is given as Eq. (24) in Box II.

From the equation for Γ_{Fu}^{BP}, we see that the paging success rate is equal to the DL LBT success probability. This means the paging success rate cannot be more than the DL LBT success probability because the channel can only be occupied when the DL LBT is successful. Following a similar analysis, we can show that paging success rate for Fast Paging with Backup POs, Γ_{Fa}^{BP}, is also ρ.

4.2.2. Paging resource usage (RU)

Let us assume that a single resource unit is used to send paging to one UE in one beam. So, the gNB uses MB resource units to send Full Paging to M UEs on B beams in $S_{Fu_M,FuB_0,Full\ PO}(0 \le M \le N)$ and $S_{Fu_0,FuB_M,Backup\ PO}(0 \le M \le N)$ states. Similarly, the gNB uses $(M+M')B$ resource units to send Full Paging to $(M+M')$ UEs on B beams in $S_{Fu_M,FuB_{M'},Backup\ PO}(0 \le M' \le N-M, 0 \le M \le N)$ states. So, the average resource units used to send Full Paging in one PO are

$$\Omega_{Fu}^{BP} = B\left(\sum_{M=0}^{N} M\ \pi_{Fu_M,FuB_0,Full\ PO} + \sum_{M=0}^{N} M\ \pi_{Fu_0,FuB_M,Backup\ PO} + \sum_{M=1}^{N}\sum_{M'=0}^{N-M}(M+M')\ \pi_{Fu_M,FuB_{M'},Backup\ PO}\right) \tag{25}$$

The gNB sends Fast Paging only on the preferred beams indicated by delay-sensitive UEs before each Full PO. If the number of delay-sensitive UEs is greater than the number of beams (i.e., $N' > B$), then the gNB may receive an indication for all the beams in the system. So, Fast Paging may be required on maximum B beams. Otherwise, the gNB can receive an indication on maximum N' beams. So, Fast Paging may be required on maximum N' beams. Thus, the maximum number of beams used for Fast Paging transmission is given by $min(B,N')$. Therefore, the maximum resource units used to send Fast Paging in one

$$
\begin{aligned}
\Gamma_{Fu}^{BP} &= \rho\Bigg(\sum_{M=0}^{N}\sum_{M'=0}^{N-M} \pi_{Fu_M,FuB_0,Full\ PO}\ {}^{N-M}\mathrm{C}_{\mathrm{M}'}\left(1-\mathrm{e}^{-\lambda(\mathrm{T}-\mathrm{T_B})}\right)^{\mathrm{M}'}\ \left(\mathrm{e}^{-\lambda(\mathrm{T}-\mathrm{T_B})}\right)^{\mathrm{N-M-M}'} + \\
&\quad \sum_{M=0}^{N}\sum_{M'=0}^{N-M}\sum_{M''=0}^{N-M-M'} \pi_{Fu_M,FuB_{M'},Backup\ PO}\ {}^{N-M-M'}\mathrm{C}_{\mathrm{M}''}\left(1-\mathrm{e}^{-\lambda\mathrm{T_B}}\right)^{\mathrm{M}''}\ \left(\mathrm{e}^{-\lambda\mathrm{T_B}}\right)^{\mathrm{N-M-M}'-\mathrm{M}\varepsilon}\Bigg) \\
&= \rho\Bigg(\sum_{M=0}^{N} \pi_{Fu_M,FuB_0,Full\ PO}\sum_{M'=0}^{N-M} {}^{N-M}\mathrm{C}_{\mathrm{M}'}\left(1-\mathrm{e}^{-\lambda(\mathrm{T}-\mathrm{T_B})}\right)^{\mathrm{M}'}\ \left(\mathrm{e}^{-\lambda(\mathrm{T}-\mathrm{T_B})}\right)^{\mathrm{N-M-M}'} + \\
&\quad \sum_{M=0}^{N}\sum_{M'=0}^{N-M} \pi_{Fu_M,FuB_{M'},Backup\ PO}\sum_{M''=0}^{N-M-M'} {}^{N-M-M'}\mathrm{C}_{\mathrm{M}''}\left(1-\mathrm{e}^{-\lambda\mathrm{T_B}}\right)^{\mathrm{M}''}\ \left(\mathrm{e}^{-\lambda\mathrm{T_B}}\right)^{\mathrm{N-M-M}'-\mathrm{M}\varepsilon}\Bigg) \\
&= \rho\Bigg(\sum_{M=0}^{N} \pi_{Fu_M,FuB_0,Full\ PO}\left(1-e^{-\lambda(T-T_B)}+e^{-\lambda(T-T_B)}\right)^{N-M} + \\
&\quad \sum_{M=0}^{N}\sum_{M'=0}^{N-M} \pi_{Fu_M,FuB_{M'},Backup\ PO}\left(1-e^{-\lambda T_B}+e^{-\lambda T_B}\right)^{N-M-M'}\Bigg) \\
&= \rho\Bigg(\sum_{M=0}^{N} \pi_{Fu_M,FuB_0,Full\ PO} + \sum_{M=0}^{N}\sum_{M'=0}^{N-M} \pi_{Fu_M,FuB_{M'},Backup\ PO}\Bigg) \\
&= \rho. \qquad (24)
\end{aligned}
$$

Box II.

PO are

$$
\begin{aligned}
\Omega_{Fa}^{BP} = min(B,N')\Bigg(&\sum_{M=0}^{N'} M\ \pi_{Fa_M,FaB_0,Full\ PO} + \\
&\sum_{M=0}^{N'} M\ \pi_{Fa_0,FaB_M,Backup\ PO} + \\
&\sum_{M=1}^{N'}\sum_{M'=0}^{N'-M} (M+M')\ \pi_{Fa_M,FaB_{M'},Backup\ PO}\Bigg) \qquad (26)
\end{aligned}
$$

4.2.3. Average paging delay

The paging delay experienced by a UE is defined in the same way as in Section 4.1.3. Fig. 4(b) illustrates the paging delay experienced by the UE in Full Paging with Backup POs. For Full Paging, if the paging is successful at the first, the second, or the third transmission attempt, the paging delay is $\delta\ \rho$, $(\delta+T_B)\ (1-\rho)\ \rho$, or $(\delta+T)\ (1-\rho)^2\rho$, respectively. Since the gNB attempts to page the UE until the paging request is sent successfully, the average paging delay is expressed as

$$
\begin{aligned}
\Delta_{Fu}^{BP} &= \sum_{k=0}^{\infty}(\delta+kT)(1-\rho)^{2k}\rho + \\
&\quad \sum_{k=0}^{\infty}(\delta+kT+T_B)(1-\rho)^{2k+1}\rho \\
&= \delta\rho\sum_{k=0}^{\infty}(1-\rho)^{2k} + T\rho\sum_{k=0}^{\infty}k(1-\rho)^{2k} + \\
&\quad (\delta+T_B)\rho(1-\rho)\sum_{k=0}^{\infty}(1-\rho)^{2k} + \\
&\quad T\rho(1-\rho)\sum_{k=0}^{\infty}k(1-\rho)^{2k}. \qquad (27)
\end{aligned}
$$

Since $\sum_{k=0}^{\infty}(1-\rho)^{2k} = \frac{1}{(2-\rho)\rho}$ and $\sum_{k=0}^{\infty}k(1-\rho)^{2k} = \frac{(1-\rho)^2}{(2-\rho)^2\rho^2}$, the expression for Δ_{Fu}^{BP} is simplified as

$$
\Delta_{Fu}^{BP} = \delta + \frac{(1-\rho)^2}{(2-\rho)\rho}T + \frac{1-\rho}{2-\rho}T_B. \qquad (28)
$$

Assuming that δ is uniformly distributed in $[0,T]$ and substituting δ with its average value of $T/2$, the expression for Δ_{Fu}^{BP} is simplified as

$$
\Delta_{Fu}^{BP} = \frac{\rho^2-2\rho+2}{2\rho(2-\rho)}T + \frac{1-\rho}{2-\rho}T_B. \qquad (29)
$$

From the above equation, it is seen that the average paging delay depends on the Full Paging cycle, the DL LBT success probability, and the time-difference between Full PO and Backup PO. The average paging delay for Fast Paging with Backup Paging is similarly expressed as

$$
\Delta_{Fa}^{BP} = \frac{\rho^2-2\rho+2}{2\alpha\rho(2-\rho)}T + \frac{1-\rho}{2-\rho}T_B. \qquad (30)
$$

4.3. Model for baseline and proposed paging schemes

As shown in Fig. 1(b), our proposed paging mechanism consists of both Full Paging and Fast Paging, along with their Backup POs (FF_BP). We compare our proposed model with three baseline paging mechanisms:

1. $NR-U$: In NR-U paging mechanism, as standardized by 3GPP, the UE wakes up periodically in the PO of the PF to receive paging. Since the gNB is equipped with directional antennas, 3GPP has specified that the PO can consist of multiple time slots and paging can be transmitted by beam sweeping over the time slots. Thus, in order to receive the paging transmitted using beam sweeping, the UE has to monitor a large number of time slots, which directly increases the overhead for the gNB due to beam sweeping and average paging delay [3]. $NR-U$ mechanism is the same as Full Paging without Backup POs analyzed in Section 4.1.
2. $NR-U_BP$: In NR-U, the channel access has to follow the LBT procedure before transmission. These transmissions are subjected to LBT failure. Authors in [21] propose an improvement to NR-U paging mechanism by providing Backup POs to the UE to cope with the possible DL LBT failure. To avoid continuous listening to the backup paging opportunities, paging monitoring can be suspended for a UE if the LBT is successful, and the paging is not intended for the UE. $NR-U_BP$ mechanism is analyzed in Section 4.2.

3. FF_noBP: 3GPP has specified that the paging can be transmitted by beam sweeping, considering the directional nature of the gNB antennas. The beam sweeping directly increases the resource overhead for the gNB and paging delay. In this regard, authors in [27] propose the concept of Full Paging and Fast Paging, where the paging message is transmitted on all beams for all (general as well as delay-sensitive) UEs and on selected beams for delay-sensitive UEs, respectively. The delay-sensitive UEs report their beam information before each Full Paging cycle. We evaluate the performance of FF_noBP mechanism by combining the analysis for Full Paging and Fast Paging in Section 4.1. Since Fast Paging is used for $N' = \sigma N$ UEs, we calculate paging success rate (Γ_{FF_noBP}) and average paging delay (Δ_{FF_noBP}) for FF_noBP by taking a weighted average of the Full Paging and Fast Paging values. These two metrics are respectively given by:

$$\Gamma_{FF_noBP} = (1-\sigma)\Gamma_{Fu} + \sigma\Gamma_{Fa} = \rho. \tag{31}$$

$$\begin{aligned}\Delta_{FF_noBP} &= (1-\sigma)\Delta_{Fu} + \sigma\Delta_{Fa} \\ &= (1-\sigma)\left(\frac{T}{\rho} - \frac{T}{2}\right) + \frac{\sigma}{\alpha}\left(\frac{T}{\rho} - \frac{T}{2}\right) \\ &= \left(1 - \sigma + \frac{\sigma}{\alpha}\right)\left(\frac{T}{\rho} - \frac{T}{2}\right).\end{aligned} \tag{32}$$

We note that there is 1 Full PO and $(\alpha - 1)$ Fast POs in 1 Full Paging cycle. Thus, paging RU (Ω_{FF_noBP}) for FF_noBP is given by

$$\Omega_{FF_noBP} = \frac{\Omega_{Fu} + (\alpha-1)\Omega_{Fa}}{\alpha}. \tag{33}$$

4. FF_BP: We evaluate the performance of our proposed FF_BP mechanism by combining the analysis for Full Paging and Fast Paging in Section 4.2. Using the same reasoning as used for FF_noBP mechanism, paging success rate (Γ_{FF_BP}), average paging delay (Δ_{FF_BP}), and paging RU (Ω_{FF_BP}) for our proposed paging mechanism FF_BP are respectively given by

$$\Gamma_{FF_BP} = (1-\sigma)\Gamma_{Fu}^{BP} + \sigma\Gamma_{Fa}^{BP} = \rho. \tag{34}$$

$$\begin{aligned}\Delta_{FF_BP} &= (1-\sigma)\Delta_{Fu}^{BP} + \sigma\Delta_{Fa}^{BP} \\ &= (1-\sigma)\left(\frac{\rho^2 - 2\rho + 2}{2\rho(2-\rho)}T + \frac{1-\rho}{2-\rho}T_B\right) + \\ &\quad \sigma\left(\frac{\rho^2 - 2\rho + 2}{2\alpha\rho(2-\rho)}T + \frac{1-\rho}{2-\rho}T_B\right) \\ &= \left(1 - \sigma + \frac{\sigma}{\alpha}\right)\frac{\rho^2 - 2\rho + 2}{2\rho(2-\rho)}T + \frac{1-\rho}{2-\rho}T_B.\end{aligned} \tag{35}$$

$$\Omega_{FF_BP} = \frac{\Omega_{Fu}^{BP} + (\alpha-1)\Omega_{Fa}^{BP}}{\alpha}. \tag{36}$$

Note that the complexity of implementing FF_BP in real-world network scenarios is not a big deal as follows. In the FF_BP scheme, a normal paging cycle is configured for general UEs and a shorter paging cycle is configured for delay-sensitive UEs. Further, each Full and Fast PO is associated with a Backup PO. This paging cycle and Backup PO configuration is similar to the current NR-U paging configuration defined by 3GPP, so it requires only minor changes in the configuration already defined in 3GPP standards. For the Fast Paging, delay-sensitive UEs need to indicate their best beam at the beginning of each Full Paging cycle. The beam reporting period is the same as the Full Paging cycle, which is longer than the paging cycle of delay-sensitive UEs. Since only one (best) beam needs to be reported infrequently, beam reporting also has low implementation complexity in a UE. So, overall, the FF_BP scheme requires only minimal additional complexity in both a UE and a gNB.

Table 2
Performance parameters.

Parameter	Values
Cell Radius	1000 m
The Number of UEs, N	1024
Paging Cycle Duration	320 ms
Arrival Rate, λ	$\{0.01, 0.05, 0.1, 0.5, 1.0\}$ s^{-1}
Delay Sensitive Fraction, σ	$\{0.3, 0.4, 0.5, 0.6, 0.7\}$
The Number of Beams, B	$\{16, 32, 64, 128\}$ [18,28]
Full Paging cycle, T	$\{320, 640, 1280, 2560\}$ ms [17]
FPCF, α	$\{4, 8\}$
DL Success Probability, ρ	$\{0.3, 0.4, 0.5, 0.6, 0.7\}$
MCOT Time	3 ms [3,22]

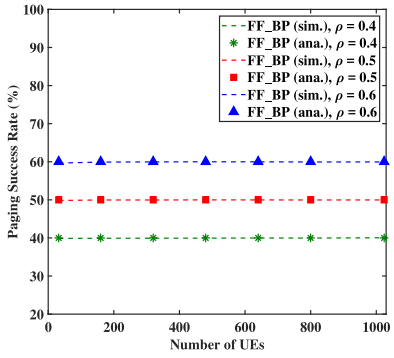

Fig. 6. Analytical results of paging success rate with varying the number of UEs in different settings.

5. Performance evaluation and simulation results

In this section, we provide the analytical and simulation results of the performance of the paging mechanisms discussed in Section 4. We first verify the analysis of our proposed paging mechanism with the simulation results. Subsequently, we compare our proposed paging mechanism with the three baseline paging mechanisms.

5.1. Simulation settings

We simulate the paging mechanisms in MATLAB, where each simulation is run for 60 min. We simulate a co-existence scenario where 30 Wi-Fi APs and a single NR-U gNB use the same unlicensed band. Table 2 shows the performance parameters in simulations. The number of WiFi APs are selected to match the DL LBT success probability of the gNB, ρ, which is in the range $\{0.4, 0.5, 0.6\}$. The UEs are randomly and uniformly deployed in a cell of radius 1000 m and their number varies from 32 to 1024. The 3GPP File Transfer Protocol (FTP) traffic model is considered to generate paging requests for each UE according to a Poisson distribution with arrival rate $\lambda \in \{0.05, 0.1, 0.5\}$ per second [29]. The maximum number of beams covering the cell, B, is selected from $\{32, 64, 128\}$ [18,28]. We consider two types of UEs: general UEs and delay-sensitive UEs, where the ratio of delay-sensitive UEs, σ, is selected from $\{0.4, 0.5, 0.6\}$. The Full Paging cycle, T, is selected from $\{320, 640, 1280, 2560\}$ ms [17] and the FPCF α, is in the range $\{4, 8\}$. The MCOT is considered as 3 ms [3,22] and so, Backup PO after Full or Fast PO occurs at $T_B = 3$ ms [21]. The gNB accesses the channel using LBT-Category 4 and while the UE accesses the channel using LBT-Category 1 [22]. According to 3GPP standards, the maximum number of target UEs in each paging message is 32 [29]. The UL success probability is always considered 1, which means UL LBT failure is not taken into account.

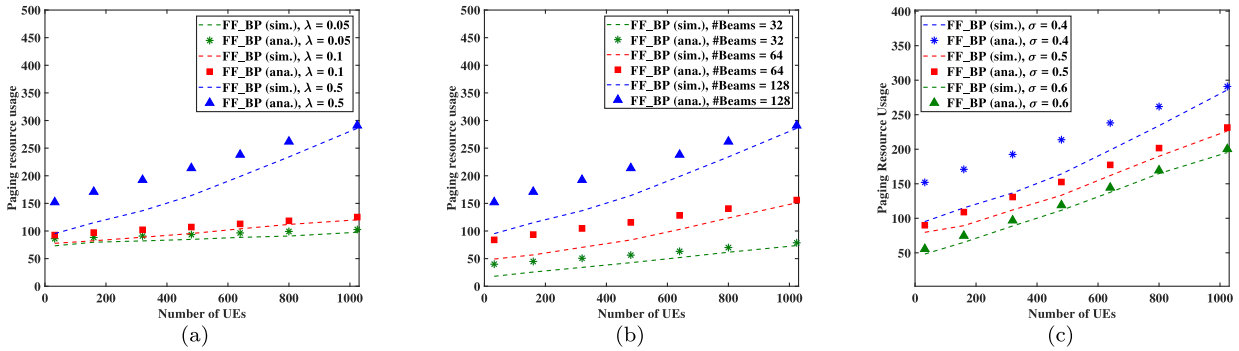

Fig. 7. Analytical results of paging resources usage with varying the number of UEs in different settings (a) Varying paging arrival rate; (b) varying the number of beams; (c) Varying delay-sensitive UE fraction.

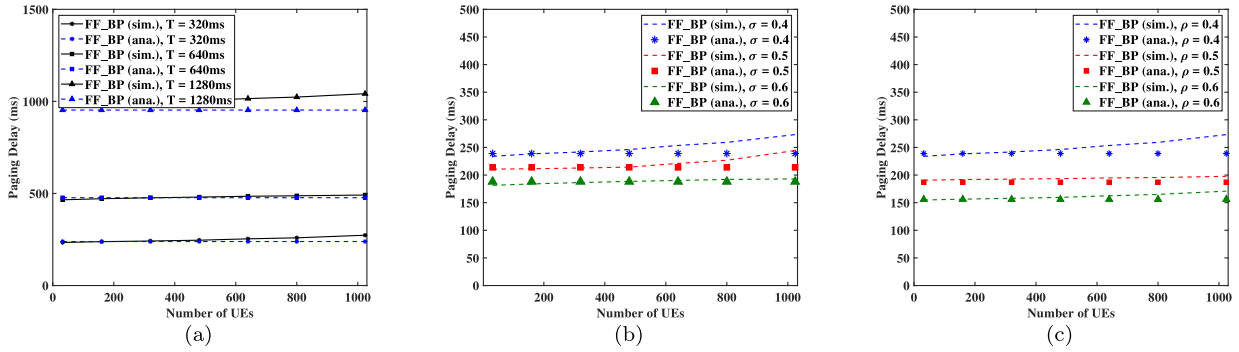

Fig. 8. Analytical results of paging delay with varying the number of UEs in different settings (a) Varying full paging cycle; (b) Varying delay-sensitive UE fraction; (c) Varying DL LBT success probability.

5.2. Results and discussion

In this section, we compare the simulation results of FF_BP with the three baseline mechanisms described in Section 4.3. In each simulation, when one parameter is varied while keeping the other parameters fixed, the following fixed values of the parameters are used: $\lambda = 0.5$, $\rho = 0.4$, $B = 128$, $\sigma = 0.4$, $\alpha = 4$, and $T = 320$ ms. For example, when λ is varied, fixed values of $\rho = 0.4$, $B = 128$, $\sigma = 0.4$, $\alpha = 4$, and $T = 320$ ms are used.

Fig. 6 demonstrates the paging success rate of FF_BP is equal to the DL LBT success probability, as derived in (34). The success rate cannot be more than DL LBT success probability because the unlicensed channel is available for transmission only when the LBT is successful.

Figs. 7(a), 7(b), and 7(c) depict the numerical results and the simulation results of paging RU of FF_BP in different settings. It is observed that the numerical results closely match the simulation results and are an upper-bound to the simulation results. It is because the numerical results assume that the maximum available number of beams in the cell are used for paging. From (36), (25), and (26), we see that paging RU increases with increasing the number of UEs, the number of beams, arrival rate, delay-sensitive UE fraction, FPCF, and decreases with increasing DL LBT success probability and Full Paging cycle. The same effect is observed in these figures as well.

Figs. 8(a), 8(b), and 8(c) illustrate the numerical and the simulation results of paging delay of FF_BP in different settings. It is observed that the simulation results closely match the numerical results. From (35), we see that the paging delay decreases with increasing delay-sensitive UE fraction, FPCF, and DL LBT success probability, and increases with increasing Full Paging cycle. The same effect is observed in these figures as well.

Fig. 9 depicts the paging RU versus the number of UEs for different paging mechanisms in different settings. Paging RU increases with increase in the number of UEs because more paging messages need to be sent. Fig. 9(a) shows the paging RU versus the number of UEs for varying the values of arrival rate λ when other parameters are fixed. Paging RU increases with increase in arrival rate because more paging messages need to be sent. Paging RU of FF_BP is less than all 3 baseline mechanisms. For example, paging resource utilization by the proposed FF_BP corresponds to 18% and 25% reduction for 0.1 and 0.5 paging arrival rate, respectively, compared to FF_noBP for 1024 UEs. FF_BP uses Fast Paging in which the less number of beams are used for paging, which in turn, reduces the resources required for paging. FF_BP also uses Backup POs with both Full and Fast Paging. This provides opportunity for more paging attempts and also, reduces the number of beams required for paging when Backup POs of Fast Paging are used.

Fig. 9(b) demonstrates the paging RU versus the number of UEs for different DL LBT success probabilities, ρ, when other parameters are fixed. FF_BP achieves lower paging RU than all 3 baseline mechanisms. For example, the paging resource utilization by the proposed FF_BP corresponds to 75% and 67% reduction for 0.4 and 0.6 DL LBT success probabilities, respectively, compared to $NR-U$ for 1024 UEs. Paging RU decreases with increase in ρ because fewer LBT failures occur and therefore, fewer Backup POs are required. Fig. 9(c) shows the paging RU versus the number of UEs for varying the maximum number of beams, B, used by the gNB, when other parameters are fixed. FF_BP achieves lower paging RU than all 3 baseline mechanisms. For example, the proposed scheme uses 34% and 25% lesser resources for 32 and 128 beams, respectively, when compared to FF_noBP. As B is increased, the number of POs on which the gNB needs to send paging also increases for both Full Paging as well as Fast Paging. Thus, the paging RU also increases with increase in B.

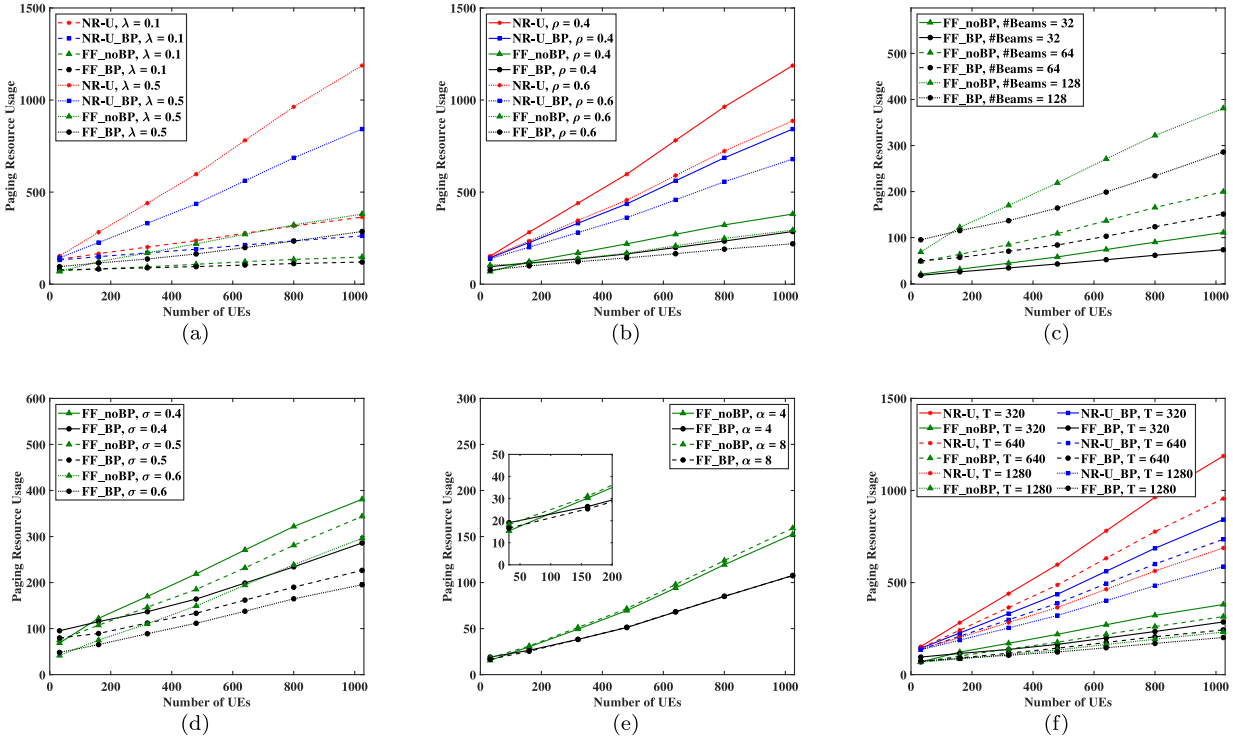

Fig. 9. Simulation results of paging resource usage with varying the number of UEs in different settings (a) Varying paging arrival rate; (b) Varying DL LBT success probability; (c) varying the number of beams; (d) Varying delay-sensitive UE fraction; (e) Varying fast paging cycle factor; (f) Varying full paging cycle.

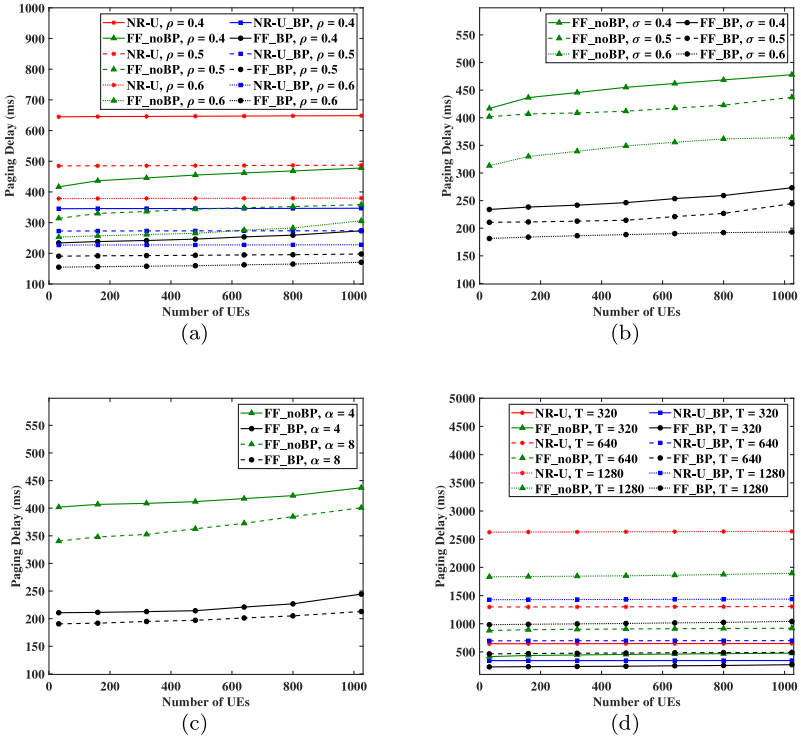

Fig. 10. Simulation results of paging delay with varying the number of UEs in different settings (a) Varying DL LBT success probability; (b) Varying delay-sensitive UE fraction; (c) Varying fast paging cycle factor; (d) Varying full paging cycle.

Fig. 9(d) delineates the paging RU versus the number of UEs for different delay-sensitive UE fractions, σ, when other parameters are fixed. FF_BP achieves lower paging RU than all 3 baseline mechanisms. For example, the proposed scheme uses 25% and 34% lesser resources for 0.4 and 0.6 delay-sensitive UE fractions, respectively, when compared to FF_noBP for 1024 UEs. Paging RU decreases with increase in σ because more paging messages are sent using Fast Paging, in which only some selected beams are used for paging. Fig. 9(e) illustrates the paging RU versus the number of UEs for different FPCFs, α, when other parameters are fixed. FF_BP achieves lower paging RU than all 3

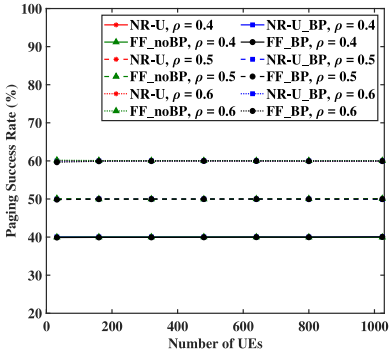

Fig. 11. Simulation results of paging success rate with varying the number of UEs in different settings.

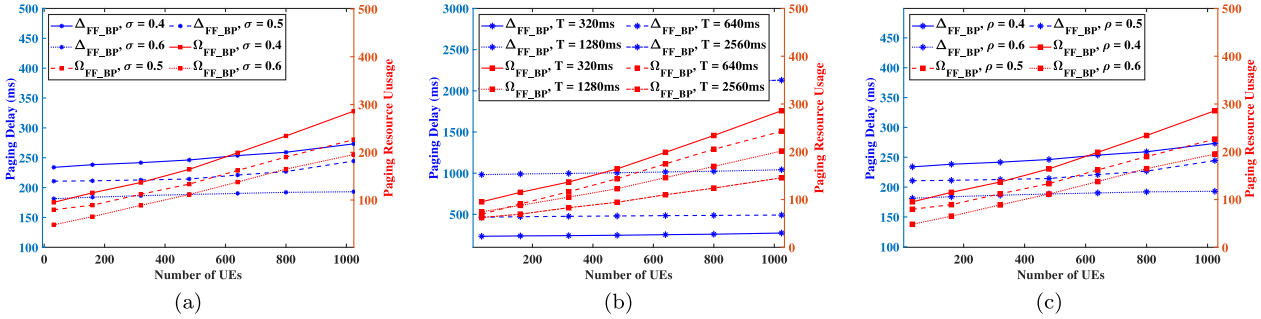

Fig. 12. Variation of paging delay and resource usage with varying the number of UEs in different settings (a) Varying delay-sensitive UE fraction; (b) Varying full paging cycle; (c) Varying DL LBT success probability.

baseline mechanisms. As α increases, there are more Fast POs per Full PO. Thus, there are more opportunities to send Fast Paging, which uses the less number of beams and so, paging RU also decreases.

Fig. 9(f) depicts paging RU versus the number of UEs for different paging cycle, when other parameters ares fixed. The proposed scheme helps to save a significant amount of paging RU when compared to the other baselines because of the Fast paging introduced between the Full paging. The Fast paging helps in reducing the paging RU by allowing paging only on the selected beams. We note that in Figs. 9(c), 9(d), and 9(e), we do not compare the results with $NR-U$ and $NR-U_BP$ mechanisms because there is no concept of Fast Paging and sending paging on selected beams for delay-sensitive UEs in these mechanisms.

Fig. 10 depicts the paging delay versus the number of UEs for different paging mechanisms in different settings. As analyzed in Sections 4.1.3 and 4.2.3, paging delay does not increase with increasing the number of UEs. It is because paging for multiple UEs (up to 32 UEs, according to 3GPP standard [29]) can be sent in 1 PO. The same effect is seen in Fig. 10 as well. Fig. 10(a) presents the paging delay versus the number of UEs for different ρ, when other parameters are fixed. A higher value of ρ means a higher probability of availability of an unlicensed channel. So, the UE has to wait less to receive the paging, thereby decreasing the paging delay. FF_BP achieves lower paging delay than all 3 baseline mechanisms. It is because FF_BP provides Backup POs for paging transmission, in case of LBT failure, and also supports Fast Paging cycles to serve delay-sensitive UEs.

Fig. 10(b) shows the paging delay versus the number of UEs for different σ, when other parameters are fixed. FF_BP achieves lower paging delay than all 3 baseline mechanisms. For example, the proposed scheme experience 43% and 46% lesser delay for 0.4 and 0.6 delay-sensitive UE fractions, respectively, when compared to FF_noBP for 1024 UEs. Paging delay decreases with increase in σ because Fast Paging is sent to more UEs when there are more delay-sensitive UEs, thus, decreasing the paging delay. Fig. 10(c) shows the paging delay versus the number of UEs for different α, when other parameters are fixed. FF_BP achieves lower paging delay than all 3 baseline mechanisms. Paging delay decreases with increase in α because Fast Paging cycle duration decreases with increase in α. Thus, there are more Fast POs within 1 Full Paging cycle, so more opportunities for successful paging transmission.

Fig. 10(d) shows that the delay increases with the increase in the paging cycle. This is because the UE has to wait for a longer time to receive paging messages. The proposed scheme experiences lesser delay when compared to the other baselines because of the additional backup POs. As analyzed in Section 4, paging delay depends only on T, ρ, α, and σ, but not on other parameters. Thus, we have not discussed the variation of paging delay with other parameters.

Fig. 11 shows the paging success rate versus the number of UEs for different paging mechanisms with varying ρ. Since paging message is not discarded after LBT failure, the paging success rate is the same as ρ, as shown in Fig. 11. The proposed scheme experiences 45% and 44% lower delay for 0.4 and 0.6 DL LBT success probabilities, respectively, when compared to FF_noBP for 1024 UEs. As analyzed in Section 4, paging success rate depends only on ρ but not on other parameters. Thus, we have not shown the variation of paging success rate with other parameters.

Figs. 12(a), 12(b), and 12(c) show the paging delay as well as the paging RU versus the number of UEs for varying delay-sensitive UE fractions (σ), varying Full Paging Cycles (T), and varying DL LBT Success Probability (ρ), respectively, when all other parameters are fixed. In all three cases, it is seen that paging delay increases only slightly even when paging RU increases sharply due to increasing the number of UEs. Increase in paging RU is expected because the number of paging messages sent by gNB increases with increase in the number of UEs. However, since paging messages are broadcasted and can be sent to several UEs at once, paging delay is not much affected by increase in the number of UEs. Thus, Fig. 12 shows that FF_BP

achieves almost fixed paging delay even as paging RU increases due to increase in the number of paging messages to be sent.

In summary, we evaluated our proposed NR-U paging mechanism and the baseline mechanisms for a wide range of parameters such as paging arrival rate, the number of beams used by the gNB, delay-sensitive UE fraction, FPCF, DL LBT success probability, and Full Paging cycle. In our evaluation, we observed that our proposed paging mechanism outperforms the baseline mechanisms in all the settings. Therefore, it is concluded that our proposed mechanism outperforms the legacy NR-U paging and the other baseline mechanisms.

6. Conclusion

In this paper, we propose an NR-U paging mechanism, FF_BP, consisting of Full and Fast Paging Cycles with Backup POs. We consider Fast POs between Full POs to quickly page delay-sensitive UEs. We also consider Fast Paging on selected beams in order to reduce a gNB's paging resource usage. We introduce Backup POs to deal with impairments of LBT procedure failure. We model the proposed paging mechanism as a discrete-time semi-Markov model and evaluate its performance in terms of paging success rate, average paging delay, and paging resource usage. We compare the proposed model with three baseline mechanisms and conclude that the proposed model has a lower paging delay and paging resource usage than the baseline mechanisms, while maintaining the same paging success rate. As future work, we will consider a scenario where the paging message is discarded after a few failed transmission attempts. In this scenario, we will evaluate the impact of such a transmission failure on the paging delay and paging success rate. We will also study the power saving of the UE by using the intermittent sleep state which the UE is not communicating with the gNB.

CRediT authorship contribution statement

Eshita Rastogi: Writing – original draft, Visualization, Validation, Software, Investigation, Formal analysis, Data curation, Conceptualization. **Abhishek Roy:** Writing – review & editing, Supervision, Conceptualization. **Ayush Rastogi:** Writing – original draft, Validation, Methodology, Formal analysis, Data curation, Conceptualization. **Jaehoon (Paul) Jeong:** Writing – review & editing, Supervision, Project administration. **Navrati Saxena:** Writing – review & editing, Supervision, Investigation, Conceptualization.

Declaration of competing interest

The authors declare the following financial interests/personal relationships which may be considered as potential competing interests: Jaehoon Jeong reports financial support was provided by National Research Foundation of Korea (NRF) and Institute of Information & Communications Technology Planning & Evaluation (IITP). If there are other authors, they declare that they have no known competing financial interests or personal relationships that could have appeared to influence the work reported in this paper.

Data availability

Data will be made available on request.

Acknowledgments

This work was supported by the National Research Foundation of Korea (NRF) grant funded by the Korea government, Ministry of Science and ICT (MSIT) (No. 2023R1A2C2002990). This work was supported in part by the Institute of Information & Communications Technology Planning & Evaluation (IITP) grant funded by the Korea MSIT (No. RS-2022-II221199, Regional strategic industry convergence security core talent training business).

References

[1] Sandra Lagen, Lorenza Giupponi, Sanjay Goyal, Natale Patriciello, Biljana Bojović, Alpaslan Demir, Mihaela Beluri, New radio beam-based access to unlicensed spectrum: Design challenges and solutions, IEEE Commun. Surv. Tutor. 22 (1) (2019) 8–37.

[2] Nhu-Ngoc Dao, Ngo Hoang Tu, Trong-Dai Hoang, Tri-Hai Nguyen, Luong Vuong Nguyen, Kyungchun Lee, Laihyuk Park, Woongsoo Na, Sungrae Cho, A review on new technologies in 3GPP standards for 5G access and beyond, Comput. Netw. (2024) 110370.

[3] Technical Specification Group Radio Access Network; Study on NR-Based Access to Unlicensed Spectrum, Technical Report TR 38.889, 3GPP, 2018.

[4] Technical Specification Group Radio Access Network; Study on New Radio Access Technology; Radio Interface Protocol Aspects, Technical Report TR 38.804, 3GPP, 2017.

[5] Ericsson mobility report, 2023, https://www.ericsson.com/en/reports-and-papers/mobility-report.

[6] Qilei Ren, Bingying Wang, Jun Zheng, Yuan Zhang, Performance modeling of an NR-U and WiFi coexistence system using the NR-U category-4 LBT procedure and WiFi DCF mechanism in the presence of hidden nodes, IEEE Trans. Veh. Technol. (2023).

[7] Natale Patriciello, Sandra Lagén, Biljana Bojović, Lorenza Giupponi, NR-U and IEEE 802.11 technologies coexistence in unlicensed mmwave spectrum: Models and evaluation, IEEE Access 8 (2020) 71254–71271.

[8] Natale Patriciello, Sanjay Goyaly, Sandra Lagen, Lorenza Giupponi, Biljana Bojovic, Alpaslan Demir, Mihaela Beluri, NR-U and WiGig coexistence in 60 GHz bands, 2020, arXiv preprint arXiv:2001.04779.

[9] Xiaowen Ye, Qian Zhou, Liqun Fu, Deep reinforcement learning-based scheduling for NR-U/WiGig coexistence in unlicensed mmWave bands, IEEE Trans. Wireless Commun. 23 (1) (2023) 58–73.

[10] John Verboom, Seungmo Kim, Stochastic analysis on downlink performance of coexistence between WiGig and NR-U in 60 GHz band, 2020, arXiv preprint arXiv:2003.01570.

[11] Yuan Gao, Zitian Zhang, Haonan Hu, Xiaoyong Wang, Yanliang Jin, Xiaoli Chu, Fair and efficiency coexistence between NR-U and WiGig networks enabled by a matching-based framework with forbidden pairs, IEEE Trans. Veh. Technol. 72 (9) (2023) 11814–11827.

[12] Mukesh Kumar Maheshwari, Eshita Rastogi, Abhishek Roy, Navrati Saxena, Dong Ryeol Shin, DRX in NR unlicensed for B5G wireless: Modeling and analysis, IEEE Trans. Mob. Comput. (2022).

[13] Eshita Rastogi, Mukesh Kumar Maheshwari, Abhishek Roy, Navrati Saxena, Dong Ryeol Shin, Machine learning-based DRX mechanism in NR-unlicensed, IEEE Wireless Commun. Lett. 11 (5) (2022) 1052–1056.

[14] Navrati Saxena, Abhishek Roy, Mukesh Kumar Maheswari, Eshita Rastogi, Dong Ryeol Shin, DRX in new radio unlicensed: A step beyond 5G wireless, IEEE Commun. Mag. 59 (1) (2021) 82–88.

[15] Mohammed Hirzallah, Marwan Krunz, Balkan Kecicioglu, Belal Hamzeh, 5G new radio unlicensed: Challenges and evaluation, IEEE Trans. Cognit. Commun. Netw. (2020).

[16] Mounika Siluveru, Dharavath Nanda, Madhavi Kesoju, Evaluation of OFDM system in terms of PAPR and BER using PAPR reduction techniques: Windowing and clipping, Babylonian J. Netw. 2024 (2024) 1–8.

[17] Kuang-Hsun Lin, Chung-Wei Weng, Hung-Yu Wei, Intelligent directional paging framework in millimeter-wave 5G NR systems, IEEE Trans. Wireless Commun. 21 (12) (2022) 10739–10754.

[18] Sanjay Goyal, Hussain Elkotby, Ravikumar Pragada, Tanbir Haque, Reducing the paging overhead in highly directional systems, in: 2021 IEEE 93rd Vehicular Technology Conference, VTC2021-Spring, IEEE, 2021, pp. 1–7.

[19] Mai-Anh Phan, Peter Alriksson, Henning Wiemann, Paging in unlicensed spectrum. U.S. Patent US11343792B2.

[20] Andrei Radulescu, Tao Luo, Chirag Patel, Methods and apparatus for paging in unlicensed communication channels. U.S. Patent US20170230933A1.

[21] Abhishek Roy, Chia-Chun Hsu, Backup paging opportunities in new radio unlicensed. U.S. Patent US11265845B2.

[22] Roberto Maldonado, Claudio Rosa, Klaus I. Pedersen, A fully coordinated new radio-unlicensed system for ultra-reliable low-latency applications, in: 2020 IEEE Wireless Communications and Networking Conference, WCNC, IEEE, 2020, pp. 1–6.

[23] Qilei Ren, Jun Zheng, Jie Xiao, Yuan Zhang, Performance analysis of an LAA and WiFi coexistence system using the LAA category-4 LBT procedure with gap, IEEE Trans. Veh. Technol. 70 (8) (2021) 8007–8018.

[24] Giuseppe Bianchi, Performance analysis of the IEEE 802.11 distributed coordination function, IEEE J. Sel. Areas Commun. 18 (3) (2000) 535–547.

[25] Vlad Stefan Barbu, Nikolaos Limnios, Semi-Markov Chains and Hidden Semi-Markov Models Toward Applications: Their Use in Reliability and DNA Analysis, vol. 191, Springer Science & Business Media, 2009.

[26] Jacques Janssen, Raimondo Manca, Applied Semi-Markov Processes, Springer Science & Business Media, 2006.

[27] Chung-Wei Weng, Biswa PS Sahoo, Ching-Chun Chou, Hung-Yu Wei, Efficient beam sweeping paging in millimeter wave 5G networks, in: 2018 IEEE International Conference on Communications Workshops, ICC Workshops, IEEE, 2018, pp. 1–6.
[28] Mamta Agiwal, Anil Agiwal, Mukesh Kumar Maheshwari, Shapna Muralidharan, Split PO for paging in B5G networks, J. Netw. Comput. Appl. 205 (2022) 103430.
[29] Technical Specification Group Radio Access Network; NR; Radio Resource Control (RRC) Protocol Specification, Technical Specification TR 38.331, 3GPP, 2020.

Eshita Rastogi is currently working as a Postdoctoral researcher at SKKU, South Korea. She received her Ph.D. degree from SKKU, M.S. degree from MMMUT, India. Her research interests include NB-IoT, NR/NR-U wireless networks, and energy efficient networks.

Abhishek Roy is currently working as a Senior Technical Manager in Wireless Standards Team of MediaTek USA Inc. Prior to this he worked as Principal Engineer in Network System Design Lab, Samsung Electronics, Korea. He received his Ph.D. in 2010 from Sungkyunkwan University, Korea and M.S. in 2002 from the University of Texas at Arlington, USA. His research interests include resource and energy management in 5G wireless, IoT, social networking and smart grids.

Ayush Rastogi is currently working as a Staff Engineer in Network System Design Lab, Samsung Electronics, Korea. He received his M.S. in 2013 from Seoul National University, South Korea and B.S. in 2011 from I.I.T. Roorkee, India. His research interests include energy-saving in IoT, resource management in 5G wireless networks, and applications of AI/ML to wireless communication.

Jaehoon (Paul) Jeong received the B.S. degree from the Department of Information Engineering, Sungkyunkwan University, in 1999, the M.S. degree from the School of Computer Science and Engineering, Seoul National University, in 2001, and the Ph.D. degree from the Department of Computer Science and Engineering, University of Minnesota, in 2009. He is currently a Professor with the Department of Computer Science and Engineering, Sungkyunkwan University. His research interests include vehicular networks, network security, intent-based networking, and cloud computing.

Navrati Saxena is an Associate Professor in Computer Science Department, San Jose State University (SJSU), USA. Prior to joining SJSU, she was an Assistant and Associate Professor in SKKU, South Korea. She completed her Ph.D. in the Department of Information and Telecommunication, University of Trento, Italy. Her prime research interests involve 5G/6G wireless, IoT, and vehicular communications. She has co-authored one book and published 80 international IEEE journals and many international conferences.